Analysis of time-of-arrival observations performed during ELF/VLF wave generation experiments at HAARP

S. Fujimaru[1] and R. C. Moore[1]

[1]   Modulated high frequency (HF) heating of the lower ionosphere in the presence of auroral electrojet currents has become an important method for generating electromagnetic waves in the extremely-low frequency (ELF) and very-low frequency (VLF) bands. Recent research efforts focus on improving the efficiency of ELF/VLF wave generation. One method to do so involves the spatial mapping of modulated currents that result from HF heating for comparison with HF heating models. As a first step toward providing a spatial map of the modulated ionospheric currents, we introduce time-of-arrival (TOA) observations performed during a series of experimental research campaigns conducted at the High-frequency Active Auroral Research Program (HAARP) in Gakona, Alaska. The TOA method provides a measurement of the ELF/VLF amplitude and phase detected at a ground-based receiver as a function of time, and this information may be used to estimate the distribution of ELF/VLF source currents within the HF heated region. In an effort to test and improve the TOA method, the University of Florida conducted ELF/VLF wave generation experiments using the HAARP HF transmitter under varying ionospheric conditions and using various transmission formats. In this paper, we summarize our experimental results and compare observations with the predictions of a theoretical model.

1.   Introduction

[2] Modulated high frequency (HF) heating of the *D*-region ionosphere can produce electromagnetic waves in the extremely low frequency (ELF, 3–3000 Hz) and the very low frequency (VLF, 3–30 kHz) bands when the HF-heated ionospheric region is in the vicinity of the auroral electrojet currents [e.g., *Getmantsev et al.*, 1974; *Stubbe et al.*, 1982; *Barr et al.*, 1991; *Villaseñor et al.*, 1996; *Papadopoulos et al.*, 2003; *Moore et al.*, 2007; *Cohen et al.*, 2010]. One important goal of modulated HF heating experiments is to improve the efficiency of ELF/VLF wave generation. For instance, observations of the amplitude and phase of ELF/VLF signals produced by modulated HF heating of the ionosphere have been used to study the dynamic and non-linear processes involved in high-power ionospheric heating in an effort to predict the best methods to increase ELF/VLF amplitudes [e.g., *Papadopoulos et al.*, 2003; *Moore et al.*, 2006].

[3] One important diagnostic tool that would greatly enhance the scientific understanding of ELF/VLF wave generation is an experimental measurement of the spatial distribution of ELF/VLF source region currents produced by modulated HF heating for comparison with theoretical predictions. *Payne et al.* [2007] demonstrated that interferometric measurements of single-frequency ELF/VLF tones could *not* be used to provide an accurate inversion of the spatial distribution of ELF/VLF source region currents, however. As *Payne et al.* [2007] discussed, one of the main weaknesses of the method was the uncertainty in the altitude of the source currents: the method could not place an upper limit on source region altitudes. In this paper, we discuss a new time-of-arrival (TOA) signal processing method for measuring the amplitude and phase of ELF/VLF signals observed at a receiver as a function of time. The method presented herein experimentally limits the altitude of ELF/VLF sources and is thus a step toward providing an experimental measurement of ionospheric ELF/VLF source region currents.

[4] The TOA method presented herein is similar in many regards to previous work analyzing the effective source height of ELF/VLF waves generated by modulated HF heating. *Rietveld et al.* [1989] demonstrated a method to determine the group delay of the ELF/VLF signal received on the ground as a function of modulation frequency. Measurements of ELF/VLF signals generated using a linear frequency-time modulation format were used to calculate the change in received phase per change in frequency, which is directly related to the overall group delay. Assuming the ELF/VLF source is located directly above the HF transmitter, *Rietveld et al.* [1989] calculated the 'apparent source height' of the ELF/VLF source region as a function of modulation frequency, although the application of this

[1]Department of Electrical and Computer Engineering, University of Florida, Gainesville, Florida, USA.
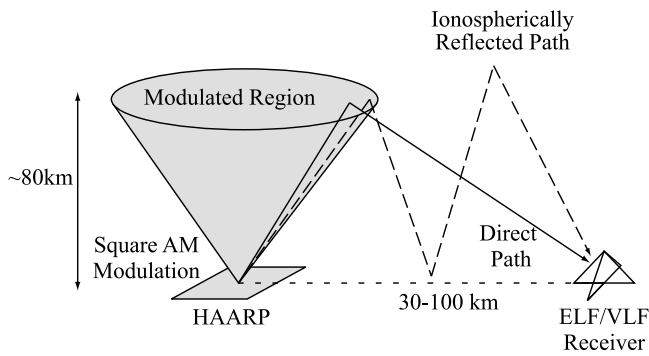
Figure 1. Cartoon diagram of the modulated HF heating beams used during our experiments. An example path of the direct and ionospherically-reflected propagations from the transmitter to the receiver are also illustrated. Our assumptions for this model are discussed in section 2.

method to experimental data produced source region altitudes varying rapidly as a function of frequency between 60 and 130 km. *Riddolls* [2003] applied a similar TOA method to ELF/VLF harmonics generated during the HF heating process, but the underlying method remained the same as that described by *Rietveld et al.* [1989].

[5] The new TOA method described in this work utilizes linear frequency-time modulation ramps, similar to the method of *Rietveld et al.* [1989], but does not directly rely upon a calculation of the measured phase differential with frequency. Instead, the presented method focuses on the calculation of an effective impulse response of the system. The time resolution attained is sufficient to distinguish between so-called direct-path ELF/VLF signals and ionospherically-reflected ELF/VLF signals, as shown in cartoon form in Figure 1, and our results indicate that ionospherically-reflected propagation paths likely affect the calculations presented by both *Rietveld et al.* [1989] and *Riddolls* [2003]. We apply this new TOA method to experimental observations performed at the High-frequency Active Auroral Research Program (HAARP) HF transmitter in Gakona, Alaska for a number of different HF transmissions. Section 2 discusses the strengths and weaknesses of the TOA method, section 3 describes the transmission formats of the experiments, and section 4 presents the experimental observations together with an analysis of the observations.

2. Time-of-Arrival Method

[6] The goal of the TOA method is to estimate the amplitude and phase of ELF/VLF waves arriving at the receiver as a function of time in such a way as to reveal characteristics of the ELF/VLF source region. As *Payne et al.* [2007] demonstrated, this is not possible using a single-tone modulation frequency. Instead, we utilize a frequency-time ramp modulation format. The frequency of the ramp varies linearly between 1 and 5 kHz over a 4-second period (1 kHz/sec slope) and repeats for approximately 3 minutes. The time-dependence of the modulation frequency provides a means to differentiate between signals arriving at different times: mixing-down the received signal using a mixing kernel with the employed frequency-time ramp format, followed by taking the discrete Fourier trans-

form (DFT) of the resulting complex signal, separates signals arriving at different times into different frequency bins. Because the frequency-time ramp is linear, the frequency bins are directly related to time of arrival. The resulting amplitudes and phases as a function of time may be interpreted as an effective impulse response for ELF/VLF wave generation. An example result of this analysis is shown in Figure 2.

[7] One main concern is the timing accuracy of the detected peak amplitude. The effective impulse response is a sampled version of the continuous impulse response convolved with a sinc function whose width is determined by the bandwidth of the transmission. While the detected peak amplitude may be interpolated in time using standard Fourier techniques, the detected peak amplitude may not exactly coincide with the timing of the actual peak amplitude incident upon the receiver, due to convolution with the sinc function. To assess this accuracy, we calculate the Cramér-Rao Lower Bound (CRLB) [*Schuster et al.*, 2006, and reference therein] using the output of a modulated HF heating model that predicts the time distribution of amplitude and phase generated by modulated HF heating of the lower ionosphere. We now describe the HF heating model and how it is used to calculate the CRLB.

[8] The HF heating model employed was developed by *Moore* [2007], and it requires as input the HF frequency, modulation frequency, and HF power. Electron temperature and density profiles, together with molecular nitrogen and molecular oxygen density profiles, are also provided as input. We apply the electron density profiles used in previous ELF/VLF studies [e.g., *Lev-Tov et al.*, 1995; *Moore*, 2007] and the rest of the ionospheric parameters are available in MSISE-90 Model provided by the Goddard Space Flight Centers Space Physics Data Facility on the web site at http://modelweb.gsfc.nasa.gov/. Using this input, the model computes the modulated conductivities (Perdersen, Hall and Parallel) at each 1 km grid in 3-D rectangular coordinates. Lastly, the model assumes a constant Electrojet electric field parallel to ground throughout the *D*-region ionosphere to
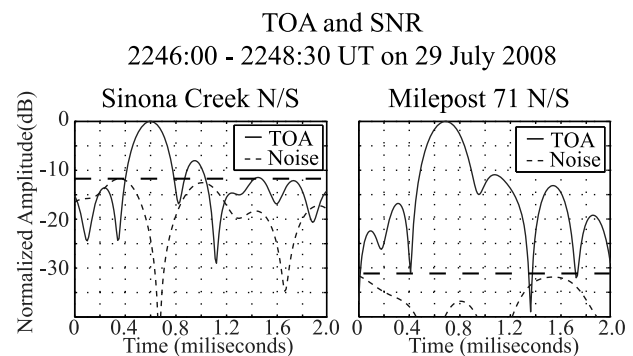
Figure 2. TOA results: The solid line shows amplitudes of the arriving VLF signals as a function of time at (left) Sinona Creek NS antenna and (right) Milepost 71 NS antenna between 2146:00 and 2148:30UT on 29 July 2008, and the dashed line shows the approximated noise level for each site. The horizontal wide dashed line is our noise reference level determined the peak approximated noise level. The reference noise level is used to estimate SNR of the detected ELF/VLF signals.

Cramer-Rao Lower Bound Time Delays
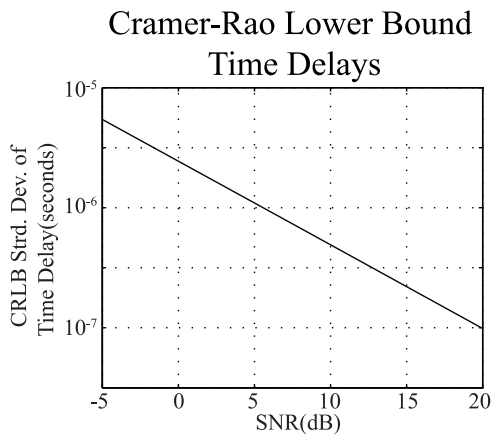
Figure 3. Cramér-Rao Lower Bound(CRLB) of the standard deviation of time delay for the peak amplitude computed by the HF heating model.

predict the magnetic field incident upon a given receiver location as a function of time assuming free-space propagation [*Payne*, 2007]. For example, the model may be used to predict the amplitude and phase magnetic field incident upon a receiver as a function of time using a modulation frequency of 2.5 kHz, an HF power of 85.7 dBW, and an HF frequency of 3.2 MHz (with X-mode polarization). The propagation model employed neglects Earth-ionosphere waveguide effects, however. For the receiver locations used in this work (each less than ~100 km away from the HAARP transmitter), this assumption is reasonable as has been demonstrated by *Payne* [2007], which showed excellent agreement between simple ray-tracing and full-wave modeling results at these distances. Applying the TOA technique to the predicted magnetic field time series, we are able to assess the timing accuracy of our peak TOA measurement. Each time bin has three unknown parameters: amplitude, phase, and time delay. We create the Fisher information matrix [*Schuster et al.*, 2006, and reference therein] which may be used to directly compute the CRLB for different white Gaussian Noise levels. Figure 3 shows the CRLB of the standard deviation of the time delay for the peak amplitude in the model as a function of the signal-to-noise ratio (SNR). Typically, the SNR of our observations is 5 dB or higher, and Figure 3 indicates a worst-case accuracy of ~1 μsec at 5 dB SNR. While model predictions using other ionospheric profiles may yield slightly different results than presented here, we expect the ~1-μsec accuracy figure to be generally representative of the accuracy of the TOA measurement. Although ELF/VLF data are also sensitive to impulsive noise (from lightning, for example) and to power line radiation in the ELF/VLF range, the CRLB is still a reasonable benchmark for timing accuracy, since the integration period is large (typically >100 seconds). In addition to the error factors discussed above, there is a 27.5 ± 2.5 μsec transmission delay due to the HAARP transmission and ±30 *n*sec GPS accuracy, which have been accounted for in our analysis.

[9] To experimentally evaluate the SNR of the measurement, we perform the same TOA analysis on the data set starting with an offset of 2 seconds. Because the frequency-time ramp is 4 seconds in duration, we do not expect

HAARP-generated ELF/VLF waves to contaminate this measurement, yielding an effective measurement of the noise floor. From among the many noise-floor measurements that the TOA analysis produces, we pick the highest noise measurement as the noise floor. As an example, Figure 2 exhibits an approximate SNR of ~12 dB (marked with a horizontal line) for the peak amplitude at Sinona Creek and an approximate SNR of ~25 dB (marked with a horizontal line) for the peak amplitude at Milepost 71, both evaluated using 2.5 minutes of data. We note that the SNR of the measurement increases significantly by repeating the frequency-time ramps for a few minutes. The Sinona Creek and Milepost 71 receivers are described in greater detail in the following section.

[10] Although the timing accuracy does not significantly limit the TOA method, the time resolution of the TOA method is a more significant factor. Timing resolution may be analyzed using standard Fourier techniques, and it is limited by the bandwidth of the received signal. For example, a signal bandwidth of 4 kHz provides a time resolution of 250 μsec, since only positive frequencies are used in the analysis. As a result, this TOA method alone cannot fully resolve signals arriving within 250 μsec of each other. Nonlinear deconvolution techniques are available and have been employed to surpass this limit, however, as will be discussed in section 4.

3. Description of Experiments

[11] TOA experiments have been performed over the course of several experimental campaigns at HAARP. During most of the campaigns, ELF/VLF wave observations were performed at two ground-based receivers located at Sinona Creek (SC) in Chistochina, Alaska (~33 km from HAARP) and at Milepost 71 (MP71) of the Tok Cutoff (~96 km from HAARP) as shown in Figure 4. During the most recent campaign in July 2010, receivers were located at
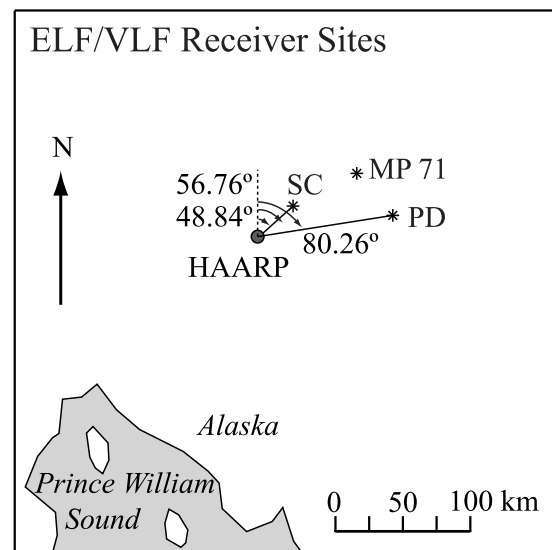
Figure 4. Geographic map showing the location of the ELF/VLF receiver sites in relation to the HAARP facility. SC refers to Sinona Creek, MP71 refers to Milepost 71 and PD refers to Paradise.

Table 1. Geomagnetic Condition[a]

Date	Time (UT)	Magnetometer (nT)	K_p Index	Riometer (dB)
29 Jul 2008	2246:00–2248:30	<25	1−	0.2
06 Aug 2009	0730:00–0755:00	<100	2+	0.5
07 Aug 2009	0645:00–0700:00	<25	2−	0.2
24 Jun 2010	2200:00–2209:30	<50	0+	0.1
22 Jul 2010	0920:00–0924:30	<50	1+	0.4

[a]Magnetometer and Riometer are located at Gakona, Alaska, and the data are available from http://www.haarp.alaska.edu/. K_p index is available from http://wdc.kugi.kyoto-u.ac.jp/kp/index.html

Sinona Creek and at Paradise (PD) (~100 km from HAARP). The receiver systems consist of air-core magnetic loop antennas oriented to detect the horizontal magnetic field at ground level, a preamplifier, a line receiver, and a digitizing computer that samples at 100 kHz with 16-bit resolution.

[12] During each of the campaigns, the HAARP HF transmitter modulated the auroral electrojet currents using square-wave amplitude modulation with linear frequency-time ramps. HF frequencies alternated between 3.2 MHz and 5.8 MHz (both with X-mode polarization) at 25%, 50% and 100% power. The modulation frequency ramps ranged from 1 kHz to 5 kHz and from 1.5 kHz to 3.5 kHz in different cases. The HF beam direction was varied: 5° off-zenith toward the receivers (56.8°), 5° off-zenith away from the receivers (236.8°), and vertical. Section 4 compares TOA results for these various transmission parameters. Geomagnetic conditions during each experiment were relatively quiet, and details are tabulated in Table 1.

4. ELF/VLF Signal Observations and Analysis

[13] In this section, we provide the TOA analysis of ELF/VLF signal observations for various scenarios. We demonstrate the TOA technique is a valid experimental measure of the received ELF/VLF signals as a function of time by comparing experimental observations with model predictions. We subsequently present TOA observations as a function of modulation format: 1) ELF/VLF modulation frequency, 2) HF beam direction, and 3) HF frequency and power.

4.1. TOA Application to Data

[14] Example TOA results are provided in Figure 2 for data acquired on 29 July 2008. During this experiment, a 7 × 7 element sub-array of the HAARP facility radiated at 3.2 MHz (X-mode) modulated with frequency-time ramps from 1 to 5 kHz over a period of 4 seconds. These frequency-time ramps were repeated sequentially for 150 seconds. Figure 2 shows the TOA result at Sinona Creek and Milepost 71 in the North-South (NS) antenna together with the approximated noise floor, demonstrating that the transmission sequence may be used to produce observations with significant SNR (~12 dB at SC and ~25 dB at MP71). Figure 5 compares these same observations with model predictions. The solid blue lines are experimental observations; the solid red traces are the predicted amplitudes as a function of time (without processing, but including ionospheric reflection); and the dashed red lines represent the

predicted amplitudes as a function of time (after TOA processing). The solid green spikes in Figure 5 are derived from observations and calculated using a nonlinear deconvolution method known as the CLEAN method [*Segalovitz and Frieden*, 1978], and the dashed green traces are the results of TOA processing on these CLEAN method extractions. The CLEAN method iteratively subtracts a portion of the largest amplitude signal from the TOA observations until the noise floor is reached. The CLEAN method thus decomposes the observed TOA into a series of complex-valued δ functions. We interpret earlier arrival times (e.g., ~573 μ seconds at SC and ~673 μ seconds at MP71) as the result of direct-path propagation, whereas we interpret later arrival times (e.g., ~900 μ seconds at SC and ~1.04 milli-seconds at MP71) as the result of ionospherically-reflected-path propagation.

[15] For Figure 5, we have selected an ionospheric profile for which the TOA of the modeled direct-path signals match the approximate TOA observed in the experimental data set for both SC and MP71. While the direct-path signals are computed as is described in section 2, for ionospherically reflected path signals, we select a reasonable reflection height and effective reflection coefficient to align predictions with the observations.

[16] The TOA of the ionospherically-reflected-path at MP71 reasonably matches model results, while at SC, the model and observations are not aligned, possibly due to the low SNR at SC data (see Figure 2). This example, and particularly the MP71 observation, demonstrates the ability of the TOA technique to discern between direct-path and ionospherically-reflected-path ELF/VLF waves observed at the receiver. It also demonstrates the ability to assign amplitude (and phase, not shown) values as a function of time. Both experimental observations and the HF heating model indicate that the time difference between the direct

TOA: Direct path vs Ionospheric Reflection
2246:00 - 2248:30 UT on 29 July 2008
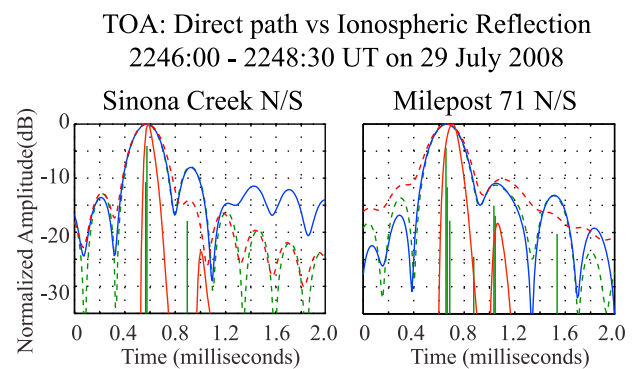
Figure 5. Comparison between modeled and observed data for (left) Sinona Creek and (right) Milepost 71; The red solid line indicates the modeled ELF/VLF signals traveling direct paths and reflected paths as the reflection height set 65 km and the effective reflection coefficient 0.3 with phase 150°. The red dashed indicates the modeled result convolve with the *sinc* function. The solid blue line indicates the observed data. The green line indicates the CLEAN method result. The green solid line is decomposed signals and dashed line is the composed signals convolved with the *sinc* function. On this plot, we use the first 10 iterations of the CLEAN method with the gain loop 0.4.
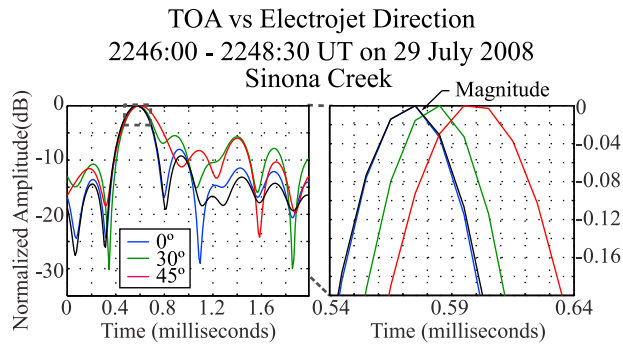
Figure 6. TOA at Sinona Creek as a function of the direction of electrojet current calculated by rotating the NS and EW antenna orientations. The fields are calculated in post-processing using $B_{rNS} = B_{NS} \cos(\theta) - B_{EW} \sin(\theta)$ where B_{NS} and B_{EW} are the magnetic fields detected using the actual antenna orientations by NS and EW respectively, and θ is the rotation angle.

and ionospherically-reflected signal paths is greater than ~400 μsec, implying a bandwidth of ~2.5 kHz is required to resolve the two peaks.

[17] Figure 5 shows the TOA analysis for only the North-South (NS) antenna, however. Due to the interference (in amplitude and phase) produced by Hall and Pedersen currents, we expect observations on the North-South (NS) and East-West (EW) antenna to be somewhat different. Furthermore, because the direction of the Hall and Pedersen currents depend on the direction of the auroral electrojet currents, we expect the time of arrival to depend on the direction of the auroral electrojet, resulting from this interference. Figure 6 shows an analysis of experimental observations. The antenna shown has been artificially rotated in post-processing to simulate the TOA variation with auroral electrojet direction. From the left panel, it is clear that the TOA analysis is dependent upon the electrojet direction (and antenna orientation). Expanding the time axis in the right panel, it is clear that even the peak arrival time depends on the electrojet direction, varying by ~30 μsec. Hence, the TOAs observed on the NS and EW antennas are determined by a combination of the magnetic fields radiated by the Hall and Pedersen currents which in turn depend on the direction of electrojet electric field. Also shown in the right hand panel (in black) is the magnitude of the TOA observation. The magnitude distribution with time does not depend on the direction of the auroral electrojet, and it represents the time of arrival for the energy the ELF/VLF wave. Throughout the remainder of this paper, we will use magnitude to represent TOA, except where noted.
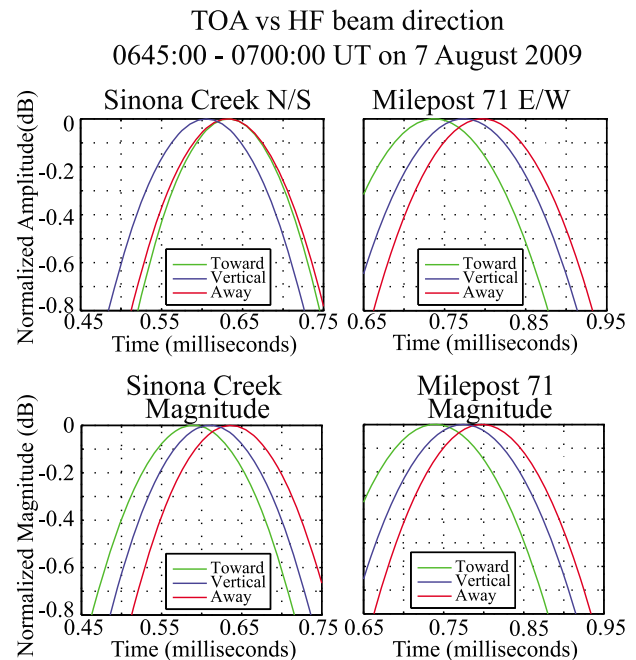
4.2. TOA Versus HF Beam Direction

[18] During the Summer Student Research Campaign (SSRC) at HAARP on August 6th and 7th, 2009, the University of Florida conducted ELF/VLF wave generation experiments to evaluate the ELF/VLF TOA as a function of HF beam direction. Unlike the TOA experiments discussed above, the modulation format consisted of frequency-time ramps ranging between 1.5 and 3.5 kHz over a period of 4 seconds (i.e., a smaller bandwidth). The HF transmitter aimed in three directions: 5° off-zenith toward Sinona

Creek, vertical, and 5° off-zenith away from Sinona Creek (azimuth 56.8°). A 5° shift in the location of the ELF/VLF source region corresponds to a ~9 km lateral offset at 100 km altitude, and only a 2–4 km difference in total ranging (from HAARP to the ionosphere to the receiver). This experiment was designed to investigate whether the TOA method is sensitive to this relatively small spatial shift. Figure 7, top, shows the TOA results for individual antennas at Sinona Creek and Milepost 71. At Milepost 71, the arrival times for each of the HF beam directions are in the order expected. At Sinona Creek, however, on the NS antenna, ELF/VLF waves generated using the vertical HF beam arrive first, followed by those generated using the "Away" beam, followed by those generated using the "Toward" beam: a very counter-intuitive result. This discrepancy results from the direction of the auroral electrojet, as discussed above. For instance, Figure 7, bottom, shows the *magnitude* of the TOA analysis and yields the intuitive result at both Sinona Creek and Milepost 71: the dominant TOA is in the order of the shortest propagation time to the longest. In addition to the ordering being correct, the TOA differences between the traces are clearly evident, indicating that the TOA method is able to detect the peak arrival time with high ranging accuracy (~2–3 km).

4.3. TOA Versus VLF Frequency

[19] During the Polar Aeronomy and Radio Science (PARS) Summer School 2010, on July 22nd, another TOA experiment was conducted to investigate the TOA of ELF/VLF waves as a function of modulation frequency. For this experiment, the full 12 × 15 element HF array broadcast at 3.25 MHz (X-mode) the frequency-time ramps ranging from 1 to 5 kHz over a period of 8 seconds (and repeated

Figure 7. TOA vs HF beam direction: TOA of a single antenna for (top left) Sinona Creek and (top right) Milepost 71 and TOA of the magnitude for (bottom left) Sinona Creek and (bottom right) Milepost 71.

TOA vs VLF Frequency
from 0920:00 - 0924:30 UT on 22 July 2010

Hall Conductivity vs Altitude
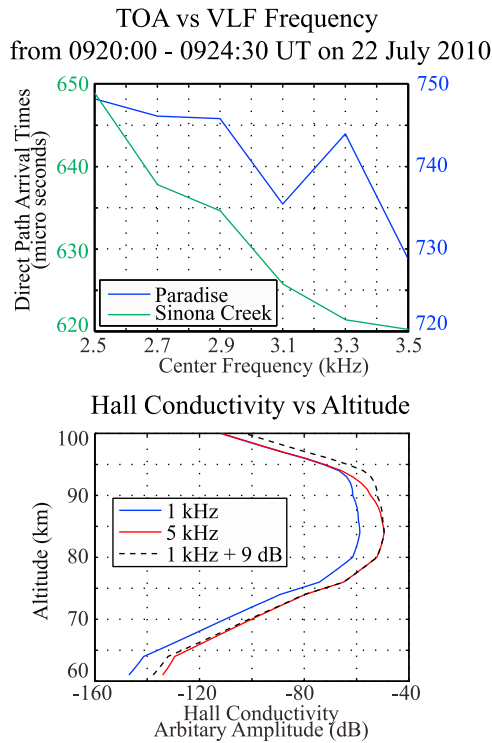
Figure 8. TOA as a function of VLF frequency (top): The Green line is the TOA for Sinona Creek and the Blue line for Paradise. Hall conductivity modulation amplitude as a function of height with different VLF frequencies (bottom): The blue line is with the VLF frequency of 1 kHz and the red line is of 5 kHz. This model is generated by using a medium electron density profile, 3.2 MHz HF frequency and full HF power with 12×15 array at HAARP.

10 times). Observations were performed at Sinona Creek and at Paradise using the TOA analysis. For this analysis, we limit the bandwidth to 3 kHz and calculate the TOA (attributed to the center frequencies of the bandwidth) for center frequencies between 2.5 and 3.5 kHz. Figure 8 shows the TOA variations as a function of center frequency for Sinona Creek and Paradise together with the modeled Hall conductivities as a function of height in Figure 8, bottom. The TOA clearly decreases with increasing center frequency at both Sinona Creek and Paradise. This relationship is not unexpected. To illustrate this effect, Figure 8, bottom, shows the altitude profile of conductivity modulation directly above the HAARP transmitter for 1 kHz and 5 kHz modulation. The variation in the two traces is almost exactly the same below 85 km altitude. Above 85 km,1 kHz modulation is relatively stronger than 5 kHz modulation. The modulation of the Pedersen conductivity (not shown) exhibits similar effects. An overall reduction in altitude with increasing modulation frequency results, and this reduction in altitude brings about a shorter propagation delay to the receiver.

4.4. TOA Versus HF Frequency and Power

[20] During the Basic Research on Ionospheric Characteristics and Effects (BRIOCHE) Campaign at HAARP in June 2010, the University of Florida conducted ELF/VLF

generation experiments to investigate the TOA as a function of HF frequency and HF power. The frequency-time ramps in this case ranged from 1 to 5 kHz over a period of 4 seconds. Every 4 seconds period, the HF power alternated between 25%, 50% and 100% power, and each period repeated for 5 minutes. Every 5 minutes, the HF frequency switched between 3.2 MHz (X-mode) and 5.8 MHz (X-mode). Observations were performed at Sinona Creek and at Milepost 71, but the introduction of commercial power lines near Milepost 71 site has significantly reduced the data quality at that site. In this section, only observations from Sinona Creek will be discussed.

[21] Figure 9 shows the TOA for the maximum peak magnitude as a function of HF power at 3.2 MHz and at 5.8 MHz. The variations in TOA are small, less than 10 μsec, whether in terms of HF frequency or in terms of HF power. The experimental results presented in Figure 9 do not definitively exhibit a monotonic increase in the TOA in terms of the HF power, and neither do they definitively show an increase in the TOA from 3.2 MHz to 5.8 MHz. Nevertheless, it is clear that the effects of HF frequency and power are relatively small compared to other parameters, such as the HF beam direction. It will be necessary to complete a full statistical analysis of HF power and HF frequency TOA observations to determine whether a consistent dependence may be derived from this data set.

5. Discussion and Summary

[22] In this paper, we have introduced a new time-of-arrival analysis method for application to ELF/VLF waves generated by modulated HF heating of the ionosphere. We have summarized TOA observations performed over the course of several HAARP campaigns and demonstrated that the TOA method is a convenient and valid experimental method to investigate the characterization of ionosphere properties and wave propagation. We demonstrated that ionospheric reflections may be discerned from direct-path elements of the ELF/VLF wave using this TOA technique, and we identified a clear dependence of the TOA on the

TOA vs HF Frequency & Power
2200:00 - 2209:30 UT on 24 June 2010
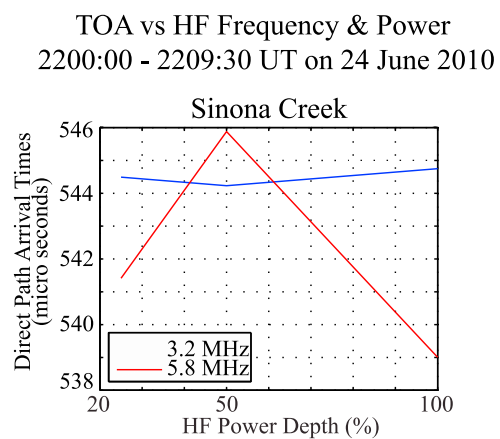
Figure 9. TOA as a function of HF frequency and power at Sinona Creek. The TOA of the maximum magnitudes is plotted as a function of HF power with different HF frequencies (blue-3.2 MHz and red-5.8 MHz). The data were taken on 24 June 2010 between 2200:00 and 2209:30 UT.

auroral electrojet direction. Furthermore, we demonstrated that application of the TOA method to experimental observations produced the expected results as a function of HF beam direction and modulation frequency. We are not able at this time to conclusively determine a clear dependence of TOA on HF power and frequency, although it may be stated that these properties have less of an effect on TOA than modulation frequency or HF beam direction. Over all, it has been demonstrated that the presented technique provides a very useful tool for the interpretation and analysis of ELF/VLF wave observations.

References

Barr, R., P. Stubbe, and H. Kopka (1991), Long-range detection of VLF radiation produced by heating the auroral electrojet, *Radio Sci.*, *26*, 871–879.

Cohen, M. B., U. S. Inan, M. Golkowski, and M. J. McCarrick (2010), ELF/VLF wave generation via ionospheric HF heating: Experimental comparison of amplitude modulation, beam painting, and geometric modulation, *J. Geophys. Res.*, *115*, A02302, doi:10.1029/2009JA014410.

Getmantsev, C. G., N. A. Zuikov, D. S. Kotik, L. F. Mironenko, N. A. Mityakov, V. O. Rapoport, Y. A. Sazonov, V. Y. Trakhtengerts, and V. Y. Eidman (1974), Combination frequencies in the interaction between high-power short-wave radiation and ionospheric plasma, *J. Exp. Theor. Phys. Lett.*, *20*, 101–102.

Lev-Tov, S. J., U. S. Inan, and T. F. Bell (1995), Altitude profiles of localized *D* region density disturbances produced in lightning-induced electron precipitation events, *J. Geophys. Res.*, *100*(A11), 21375–21383, doi:10.1029/95JA01615.

Moore, R. C. (2007), *ELF/VLF wave generation by modulated HF heating of the auroral electrojet*, Ph.D. thesis, Stanford Univ., Stanford, Calif.

Moore, R. C., U. S. Inan, and T. F. Bell (2006), Observations of amplitude saturation in ELF/VLF wave generation by modulated HF heating of the auroral electrojet, *Geophys. Res. Lett.*, *33*, L12106, doi:10.1029/2006GL025934.

Moore, R. C., U. S. Inan, T. F. Bell, and E. J. Kennedy (2007), ELF waves generated by modulated HF heating of the auroral electrojet and observed at a ground distance of 4400 km, *J. Geophys. Res.*, *112*, A05309, doi:10.1029/2006JA012063.

Papadopoulos, K., T. Wallace, M. McCarrick, G. M. Milikh, and X. Yang (2003), On the efficiency of ELF/VLF generation using HF heating of the auroral electrojet, *Plasma Phys. Rep.*, *29*, 561–565.

Payne, J. A. (2007), Spatial structure of very low frequency modulated ionospheric currents, Ph.D. thesis, Stanford Univ., Stanford, Calif.

Payne, J. A., U. S. Inan, F. R. Foust, T. W. Chevalier, and T. F. Bell (2007), HF modulated ionospheric currents, *Geophys. Res. Lett.*, *34*, L23101, doi:10.1029/2007GL031724.

Riddolls, R. J. (2003), Structure of the polar electrojet antenna, Ph.D. thesis, Mass. Inst. of Technol., Cambridge, Mass.

Rietveld, M. T., P. Stubbe, and H. Kopka (1989), On the frequency dependence of ELF/VLF waves produced by modulated ionospheric heating, *Radio Sci.*, *24*, 270–278.

Schuster, S., S. Scheiblhofer, L. Reindl, and A. Stelzer (2006), Performance evaluation of algorithms for SAW-based temperature measurement, *IEEE Trans. Ultrason. Ferroelectr. Freq. Control*, *53*, 1177–1185.

Segalovitz, A., and B. R. Frieden (1978), A "CLEAN"-type deconvolution algorithm, *Astron. Astrophys. Suppl.*, *70*, 335–343.

Stubbe, P., H. Kopka, M. T. Rietveld, and R. L. Dowden (1982), ELF and VLF generation by modulated HF heating of the current carrying lower ionosphere, *J. Atmos. Terr. Phys.*, *44*, 1123–1135.

Villaseñor, J., A. Y. Wong, B. Song, J. Pau, M. McCarrick, and D. Sentman (1996), Comparison of ELF/VLF generation modes in the ionosphere by the HIPAS heater array, *Radio Sci.*, *31*, 211–226.

S. Fujimaru, Department of Electrical and Computer Engineering, University of Florida, 320 Benton Hall, Center Drive, Gainesville, FL 32611, USA. (shuji15@ufl.edu)

R. C. Moore, Department of Electrical and Computer Engineering, University of Florida, 319 Benton Hall, Center Drive, Gainesville, FL 32611, USA. (moore@ece.ufl.edu)